AAC Journals.ASM.org

Cytostatic versus Cytocidal Activities of Chloroquine Analogues and Inhibition of Hemozoin Crystal Growth

Alexander P. Gorka,[a,b,c] John N. Alumasa,[a,b,c]* Katy S. Sherlach,[a,b,c] Lauren M. Jacobs,[a,b,c] Katherine B. Nickley,[a,b,c]* Jonathan P. Brower,[a,b,c]* Angel C. de Dios,[c] Paul D. Roepe[a,b,c]

Department of Biochemistry and Molecular & Cellular Biology,[a] Center for Infectious Diseases,[b] and Department of Chemistry,[c] Georgetown University, Washington, DC, USA

We report an improved, nonhazardous, high-throughput assay for *in vitro* quantification of antimalarial drug inhibition of β-hematin (hemozoin) crystallization performed under conditions that are more physiological relative to previous assays. The assay uses the differential detergent solubility of crystalline and noncrystalline forms of heme and is optimized via the use of lipid catalyst. Using this assay, we quantify the effect of pH on the crystal growth-inhibitory activities of current quinoline antimalarials, evaluate the catalytic efficiencies of different lipids, and test for a possible correlation between hemozoin inhibition by drugs versus their antiplasmodial activity. Consistent with several previous reports, we found a good correlation between hemozoin inhibition potency versus cytostatic antiplasmodial potency (50% inhibitory concentration) for a series of chloroquine (CQ) analogues. However, we found no correlation between hemozoin inhibition potency and cytocidal antiplasmodial potency (50% lethal dose) for the same drugs, suggesting that cellular targets for these two layers of 4-aminoquinoline drug activity differ. This important concept is also explored further for QN and its stereoisomers in the accompanying paper (A. P. Gorka, K. S. Sherlach, A. C. de Dios, and P. D. Roepe, Antimicrob. Agents Chemother. 57:365–374, 2013).

There are an estimated 350 million to 500 million *Plasmodium falciparum* malaria infections annually, with at least 1 million of these being fatal (1). The continued spread and evolution of resistance to currently used antimalarials (2–5) have generated renewed effort to design drugs effective against chloroquine (CQ)-resistant (CQR) malaria. This effort benefits from further development of rapid, inexpensive screens that more reliably estimate antiplasmodial activity.

During the trophozoite stage of the intraerythrocytic cycle, *P. falciparum* actively degrades host red blood cell hemoglobin, producing millimolar quantities of toxic ferriprotoporphyrin IX (FPIX) heme within the digestive vacuole (DV) of the parasite (6, 7). Due to the lack of a heme oxygenase pathway (8), the malarial parasite maintains a low concentration of toxic free heme by sequestration into inert, nontoxic crystalline hemozoin (Hz) (9–12). The Hz crystallization pathway is an important target for antimalarial chemotherapy. Quinoline antimalarials, such as CQ and amodiaquine (AQ), are known to bind to multiple precrystalline forms of heme in different ways and thus presumably inhibit crystal growth by sequestration of monomeric and/or dimeric heme (13–18). Quantifying drug inhibition of Hz formation *in vitro* has often been viewed as a faster and more economical way to predict and even quantify drug antiplasmodial activity *in vivo* (15, 16, 19–26). However, the assays that have been used in this manner are typically done under conditions that are far from physiological. Also, it is becoming increasingly clear that some antimalarial drugs possess both cytostatic (growth-inhibitory; quantified by use of the 50% inhibitory concentration [IC_{50}]) and cytocidal (parasite cell kill; quantified by use of the 50% lethal dose [LD_{50}]) activity. To our knowledge, no studies have tested how Hz inhibition potency is related to both IC_{50} and LD_{50}.

Although Hz crystallization chemistry is not completely elucidated, it is known that preformed Hz, certain proteins, and some lipids can facilitate heme crystallization (11, 27–29). Current evidence strongly supports lipid catalysis of crystallization *in vivo*, since lipid nanospheres have been shown to be closely associated with nascent Hz crystals within the DV of the parasite (11, 28). Also, a variety of lipids isolated from the DV of malarial parasites have been shown to efficiently catalyze Hz crystal growth *in vitro* (11, 28, 30, 31). Although the concentration and exact identity of the lipids extracted from the DV is still not fully known (11, 28), phosphatidylcholine (PC), monoacylglycerols (MAGs), diacylglycerols (DAGs), and triacylglycerols (TAGs) are among those identified to be present within this acidic compartment.

Several plate-based and non-plate-based assays have been developed to quantify Hz crystal growth and inhibition of that growth by drugs (12, 22, 23, 25, 32–37). Most previously reported assays require centrifugation and/or filtration and are performed under nonphysiological conditions (an exception being low-throughput assays performed previously [11]). Some of these studies have hinted at a correlation between Hz inhibition potency and antiplasmodial IC_{50}, but contrasting results have also been reported (19, 21, 38). We recently reported a significant correlation between Hz inhibition and IC_{50} across a series of structurally related quinine (QN) analogues (39) but found that it does not

Received 17 August 2012 **Returned for modification** 5 October 2012
Accepted 26 October 2012

Published ahead of print 31 October 2012

Address correspondence to Paul D. Roepe, roepep@georgetown.edu.

* Present address: John N. Alumasa, Department of Biochemistry & Molecular Biology, The Pennsylvania State University, University Park, Pennsylvania, USA; Katherine B. Nickley, Georgetown University School of Medicine, Washington, DC, USA; Jonathan P. Brower, Tufts University School of Medicine, Boston, Massachusetts, USA.

A.P.G. and J.N.A. contributed equally to this article.

Supplemental material for this article may be found at http://dx.doi.org/10.1128/AAC.01709-12.

doi:10.1128/AAC.01709-12

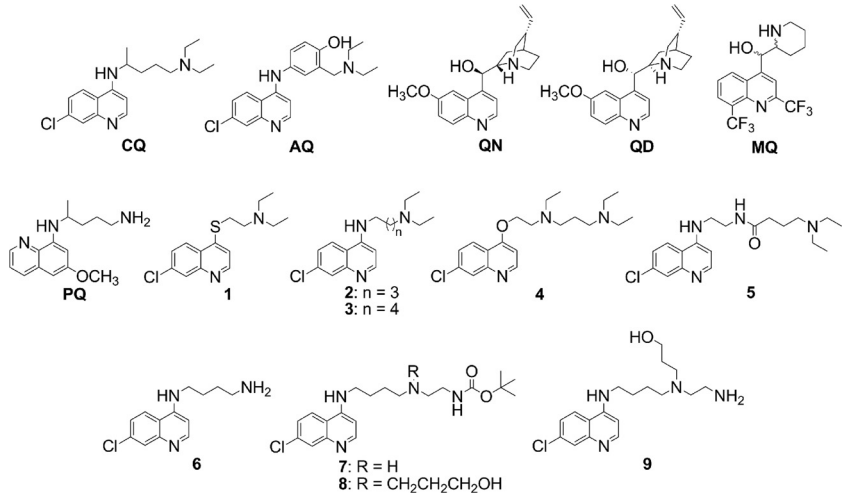

FIG 1 Structures of common quinoline antimalarials and 7-chloroquinoline drug analogues used in this study. MQ, mefloquine; PQ, primaquine.

hold when cytocidal activity (LD_{50}) is considered the antiplasmodial measurement (see the accompanying paper [40]). In previously reported high-throughput assays, multiple steps involved in the processing of Hz crystals are cumbersome and can add additional error. Some use hazardous reagents or require expensive equipment, such as microfiltration plates.

Additional development of several classes of antimalarial drugs would benefit from a more complete understanding of the relationship between drug potency against malarial parasites and their ability to inhibit Hz formation. As part of this effort, high-throughput assays that more closely mimic the physiological conditions of Hz formation would be helpful. We have developed such an assay that uses physiologically relevant lipid catalysts, ionic strength, and temperature and that incorporates inexpensive, readily attainable, nonhazardous reagents. Using this assay, we quantified the effect of pH on Hz inhibition for common antimalarials, CQ, QN, quinidine (QD), and amodiaquine (AQ), and evaluated the catalytic efficiencies of different lipids. We also tested for a correlation between Hz inhibition and antiplasmodial IC_{50} and LD_{50} for a series of CQ analogues with a wide range of antiplasmodial activities (Fig. 1) (24, 41–43).

MATERIALS AND METHODS

Materials and chemicals. Routine chemicals, media, and solvents were reagent grade or better, purchased from Sigma-Aldrich (St. Louis, MO) or Fisher Scientific (Newark, DE), and used without further purification. Sterile polystyrene 96-well tissue culture plates and other laboratory plastics were purchased from Fisher Scientific. 1-Monopalmitin (pMAG) and 1-monostearin (sMAG) were purchased from Doosan Serdary Research Laboratories (Toronto, ON, Canada). 1,2-Diolyl-*rac*-glycerol (18:1, *cis*-9) (DO), 1,2-dipalmitoyl-*sn*-glycerol-3-PC (DG), and 1,2-dioctanoyl-*sn*-glycerol-3-PC (DT) were purchased from Avanti Polar Lipids Inc. (Alabaster, AL). Kieselgel 60 silica was purchased from Selecto Scientific (Suwanee, GA). Sodium dodecyl sulfate (SDS) was purchased from Bio-Rad Laboratories (Hercules, CA). Hemin was from Fluka (Buchs, Switzerland). $CDCl_3$ was purchased from Cambridge Isotope Laboratories Inc. (Andover, MA). SYBR green I nucleic acid dye was purchased from Invitrogen (Eugene, OR).

Antimalarial drugs QN monohydrochloride dihydrate, QD hydrochloride monohydrate, CQ diphosphate, and AQ dihydrochloride dihydrate were purchased from Sigma-Aldrich. Synthesis and chemical characterization of CQ analogues 1 to 5 have been reported previously (24, 41–43). Compounds 6 to 9 were synthesized as described below.

General methods. Flash chromatography was performed on Kieselgel 60 (particle size, 0.032 to 0.063 mm). Thin-layer chromatography (TLC) analyses were performed on Selecto Scientific flexible TLC plates (silica gel 60, F 254, 200 μm). Nuclear magnetic resonance (NMR) spectra were obtained on a 400-MHz (^{1}H) and 100-MHz (^{13}C) Varian Fourier transform (FT)-NMR spectrometer (Santa Clara, CA) using $CDCl_3$ as the solvent and tetramethylsilane (TMS) as the external standard.

Synthesis of compounds 6 to 9 (Fig. 2). (i) *N*-(7-Chloro-4-quinolyl)-1,4-diaminobutane (compound 6). 4,7-Dichloroquinoline (4.0 g, 20.3 mmol) was dissolved in 1,4-diaminobutane (10.7 g, 121.4 mmol) under N_2 and heated to 80°C for 1 h, followed by 100°C for 5 h. A white precip-

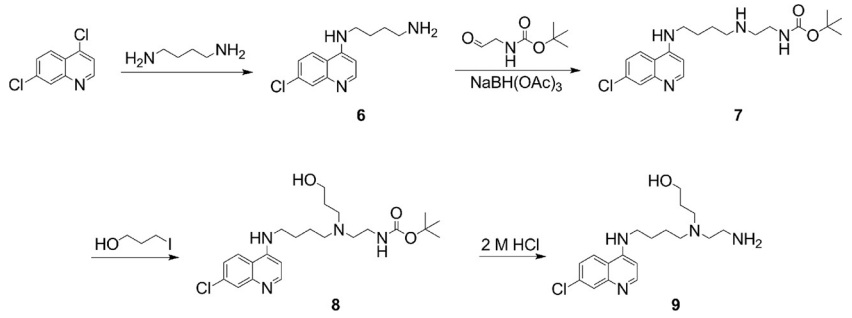

FIG 2 Synthesis of compounds 6 to 9. $NaBH(OAc)_3$, sodium triacetoxyborohydride.

itate was observed after 1 h. After cooling to room temperature, 1 M NaOH (40 ml) was added and the reaction mixture was extracted with CH_2Cl_2. The organic layer was washed with brine and H_2O, dried over anhydrous Na_2SO_4, and concentrated *in vacuo* to afford the product as a white solid (3.4 g, 13.5 mmol) in 67% yield. ^{1}H NMR (400 MHz, $CDCl_3$) δ 1.19 (bs, 2H), 1.64 (m, 2H), 1.87 (m, 2H), 2.83 (t, 2H), 3.30 (q, 2H), 6.00 (bs, 1H), 6.38 (d, 1H), 7.33 (dd, 1H), 7.73 (d, 1H), 7.94 (d, 1H), 8.52 (d, 1H). ^{13}C NMR (100 MHz, $CDCl_3$) δ 26.26, 30.99, 41.70, 43.41, 99.02, 117.55, 121.62, 125.18, 128.92, 134.82, 149.42, 150.16, 152.28.

(ii) *N*-(7-Chloro-4-quinolyl)-*N*′-(*N*″-*t*-Boc-aminoethyl)-1,4-diaminobutane (compound 7) (44). A solution of *N*-(7-chloro-4-quinolyl)-1,4-diaminobutane (compound 6; 0.9 g, 3.7 mmol), *N*-*tert*-butoxycarbonyl (*N*-*t*-Boc) glycinal (1.0 g, 6.3 mmol), and sodium triacetoxyborohydride (1.4 g, 6.7 mmol) in anhydrous CH_2Cl_2 was allowed to stir at room temperature for 24 h. The reaction was quenched by the addition of H_2O, and the organic layer was extracted with saturated $NaHCO_3$, dried over anhydrous Na_2SO_4, and concentrated *in vacuo* to give a yellow oil. This was further purified by column chromatography over silica gel (5% methanol [MeOH], CH_2Cl_2), with a gradual increase to 30% and, finally, 100% MeOH. The product eluted as a yellow oil (1.1 g, 2.7 mmol) in 75% yield. ^{1}H NMR (400 MHz, $CDCl_3$) δ 1.38 (s, 9H plus solvent peak overlap = 13H), 1.52 (m, 2H), 1.70 (m, 2H), 2.47 (m, 4H), 3.11 (m, 2H), 3.25 (m, 2H), 5.06 (bs, 1H), 5.63 (bs, 1H), 6.33 (d, 1H), 7.25 (dd, 1H), 7.79 (d, 1H), 7.78 (d, 1H), 8.42 (d, 1H). ^{13}C NMR (100 MHz, $CDCl_3$) δ 24.62, 25.98, 28.24, 38.33, 42.92, 49.90, 53.52, 79.06, 98.50, 117.01, 121.87, 124.90, 127.37, 134.78, 148.16, 150.32, 151.02, 156.19.

(iii) *N*-(7-Chloro-4-quinolyl)-*N*′-(*N*″-*t*-Boc-aminoethyl)-*N*′-(3-hydroxypropyl)-1,4-diaminobutane (compound 8) (44). A solution of *N*-(7-Chloro-4-quinolyl)-*N*′-(*N*″-*t*-Boc-aminoethyl)-1,4-diaminobutane (compound 7; 2.4 g, 6.2 mmol) and 3-iodo-1-propanol (0.6 g, 3.1 mmol) was refluxed in anhydrous CH_3CN for 8 h. The solvent was evaporated, and the resulting brownish yellow oil was taken up in CH_2Cl_2 (60 ml). This was extracted with saturated $NaHCO_3$, dried over anhydrous Na_2SO_4, and concentrated *in vacuo*. The crude oil was purified via column chromatography (5% MeOH, CH_2Cl_2), with a gradual increase to 30% MeOH. The pure product eluted as a brownish yellow oil (1.2 g, 2.7 mmol) in 86% yield. ^{1}H NMR (400 MHz, $CDCl_3$) δ 1.37 (s, 9H plus solvent peak overlap = 15H), 1.57 (m, 2H), 1.81 (m, 2H), 2.13 (m, 2H), 2.54 (m, 6H), 3.14 (m, 4H), 3.61 (m, 4H), 4.12 (bs, 1H), 5.14 (bs, 1H), 5.25 (bs, 1H), 6.69 (d, 1H), 7.51 (d, 1H), 7.82 (s, 1H), 7.94 (s, 1H), 8.62 (d, 1H). ^{13}C NMR (100 MHz, $CDCl_3$) δ 25.46, 25.74, 28.35, 30.91, 38.39, 43.35, 50.36, 51.82, 53.4, 57.48, 79.11, 98.30, 98.88, 116.72, 127.42, 127.84, 138.25, 140.73, 147.13, 155.02, 156.32.

(iv) *N*-(7-Chloro-4-quinolyl)-*N*′-(*N*″-aminoethyl)-*N*′-(3-hydroxypropyl)-1,4-diaminobutane (compound 9) (44). *N*-(7-Chloro-4-quinolyl)-*N*′-(*N*″-*t*-Boc-aminoethyl)-*N*′-(3-hydroxypropyl)-1,4-diaminobutane (compound 9; 1.2 g, 2.7 mmol) was dissolved in anhydrous MeOH (40 ml). 2 M HCl (14 ml, 28.0 mmol) was added, and the reaction was allowed to stir at room temperature for 24 h. The solvent was evaporated, and the crude product was taken up in CH_2Cl_2. This was extracted with 1 M NaOH, and the combined organic layers were dried over anhydrous Na_2SO_4 and concentrated *in vacuo* to afford the pure product (0.5 g, 1.4 mmol) in 53% yield. ^{1}H NMR (400 MHz, $CDCl_3$) δ 1.53 (m, 2H), 1.70 (m, 2H), 1.85 (m, 2H), 2.42 (m, 4H), 2.66 (m, 4H), 3.22 (t, 2H), 3.52 (t, 2H), 3.91 (t, 2H), 5.72 (t, 1H), 6.29 (d, 1H), 7.24 (d, 1H), 7.77 (d, 1H), 7.83 (d, 1H), 8.40 (d, 1H). ^{13}C NMR (100 MHz, $CDCl_3$) δ 25.13, 30.60, 39.51, 48.55, 53.49, 54.26, 57.06, 57.62, 78.89, 98.60, 98.65, 114.16, 123.15, 127.03, 136.18, 139.03, 154.30, 156.05.

Effect of SDS on absorbance of FPIX. The effect of SDS on FPIX absorbance was analyzed in two ways. First, a solution of FPIX (5 mM) was prepared in 0.1 M NaOH and diluted to 10 μM in 0.1 M bicarbonate buffer (pH 9.1), and aliquots of an SDS stock solution (50%, wt/vol; 1.734 M) were added to 1 ml of the FPIX solution in a stirred cuvette. Titration with SDS (to a final concentration of 0.5 to 5%, wt/vol) was monitored with an Agilent 8453 UV-visible spectrophotometer (Santa Clara, CA). Also, a 5 mM FPIX stock was diluted to 1 mM in 0.1 M bicarbonate buffer (pH 9.1) containing different concentrations of SDS (0, 0.5, 1.0, 2.5, and 5%, wt/vol). These solutions were then serially diluted in 1.5-μl microcentrifuge tubes such that the final FPIX concentration ranged from 0 to 20 μM. Equal volumes (200 μl) of these solutions were then transferred in triplicate to microtiter plate wells. Absorbance readings from the wells were obtained at 405 nm using a BioTek ELx800 absorbance microplate reader (Winooski, VT).

Assay optimization. The heme concentration was optimized by comparing the Hz yield upon various starting heme concentrations. The optimal concentration of catalyst was determined in the presence of 100 μM FPIX, propionate buffer (1 M) at 37°C in a 16-h assay format (see Results). We compared the Hz yield in the presence of sonicated lipids, phosphatidylserine (PS), PC, pMAG, sMAG, DO, DG, and DT, as well as mixtures of PC, pMAG, and sMAG, versus pH and at a range of lipid concentrations. PC, pMAG, and sMAG produced the highest Hz yields when used at ≥0.5 mg/ml (see Fig. S1 in the supplemental material). Additionally, catalytic efficiency was assessed at pH 5.2 versus pH 5.6 (45) in kinetic assays using PC, pMAG, or sMAG. The optimal buffer concentration was determined in the presence of 100 μM FPIX, propionate buffer (pH 5.2), and 0.5 mg/ml PC at 37°C using a 16-h assay as described below, with the greatest Hz yield achieved at 1 M propionate (see Fig. S2 in the supplemental material).

Hz inhibition assay. As described in Results, the optimized assay is based on the differential solubility of crystalline and noncrystalline forms of FPIX in 2.5% (wt/vol) SDS (86.7 mM) and alkaline bicarbonate buffer (0.1 M, pH 9.1). Hemin (2 mM) in 0.1 M NaOH was titrated to the desired pH with propionate buffer. Ten-microliter volumes from the hemin stock were then transferred to 96-well plates, followed by addition of propionate buffer (180 μl per well) and previously sonicated lipid catalyst (10 μl). Appropriate blanks and controls (e.g., no lipid catalyst, no drugs) were included in each plate. Plates were wrapped in plastic wrap and incubated at 37°C with gentle shaking. Hz yield assays were terminated after 16 h by addition of 100 μl of a solution of SDS dissolved in 0.1 M bicarbonate buffer (pH 9.1) (final concentration/well of SDS, 2.5%, wt/vol; 86.7 mM), and kinetic assays at multiple time points were quenched in a similar fashion. The well contents were gently mixed and incubated at room temperature for 10 min to allow undissolved crystals to settle. A 50-μl aliquot from each well was then transferred to a second plate preloaded with 200 μl/well of SDS solution (2.5%, wt/vol; 86.7 mM) in 0.1 M bicarbonate buffer, and the absorbance at 405 nm was read with a 96-well-plate-adapted ELx800 BioTek absorbance microplate reader.

Conversion of the absorbance values to the FPIX concentration (μM) remaining in the sample wells was done using a linear calibration curve measured for each assay. FPIX stocks ranging in concentration from 0 to 16 μM were freshly prepared in 2.5% SDS–0.1 M bicarbonate buffer (pH 9.1). Volumes of 250 μl were transferred to predesignated wells, the absorbance at 405 nm was read, and the data were fit to a straight line. Free FPIX remaining in solution (inverse of Hz produced) was quantified using equation 1:

$$[H^X] = \left[\frac{A^s_{405} - A^0_{405} - C}{\varepsilon_{405}}\right] \times D \quad (1)$$

where $[H^X]$ is the concentration of FPIX (μM) remaining, A^s_{405} and A^0_{405} are the absorbance (405 nm) readings (averages from triplicate wells) of the sample and blank, respectively, ε_{405} is the extinction coefficient for FPIX, C is a constant obtained from the fit to the calibration curve, and D is the dilution factor.

Antiplasmodial activity measurements. *P. falciparum* strains HB3 and Dd2 were obtained from the Malaria Research and Reference Reagent Resource Center (Manassas, VA). Off-the-clot, heat-inactivated pooled type O-positive human serum and O-positive human whole blood were purchased from Biochemed Services (Winchester, VA). Custom 5% O_2–5% CO_2–90% N_2 culturing gas blend was purchased from Robert's Oxygen (Rockville, MD).

All *P. falciparum* strains were maintained using the method of Trager and Jensen (46), with minor modifications. Briefly, cultures were maintained under an atmosphere containing 5% O_2, 5% CO_2, 90% N_2 gaseous mix at 2% hematocrit and 1 to 2% parasitemia in RPMI 1640 supplemented with 10% type O-positive human serum, 25 mM HEPES (pH 7.4), 23 mM $NaHCO_3$, 11 mM glucose, 0.75 mM hypoxanthine, and 20 μg/liter gentamicin with regular medium changes every 48 h. Antiplasmodial cytocidal (LD_{50}) and cytostatic (IC_{50}) activities against the chloroquine-sensitive (CQS) HB3 strain and CQR Dd2 strain were assessed. Cytostatic antiplasmodial activities have previously been reported for some drugs used in this study (24, 41–43), and additional activities were determined as described previously (47, 48), with minor modifications.

The cytocidal assay utilizes a 6-h bolus dose with high concentrations of drug, followed by washing drug away and growth in the absence of drug for 48 h, while the cytostatic assay utilizes continuous growth for 48 h in the constant presence of low concentrations of drug. Test compounds were dissolved in deionized water or dimethyl sulfoxide (DMSO). Serial drug dilutions were made using complete medium, and 100-μl aliquots were transferred to 96-well clear-bottom black plates. Following addition of 100 μl of asynchronous or sorbitol-synchronized culture (1% final parasitemia, 2% final hematocrit), plates were transferred to an airtight chamber gassed with 5% O_2–5% CO_2–90% N_2 and incubated at 37°C.

For the cytocidal assay, plates were incubated for 6 h, followed by centrifugation with an Eppendorf 5804 centrifuge fitted with an A-2-DPW rotor (Hauppauge, NY) at 700 × *g* for 3 min. Drug-containing medium was removed, and cell pellets were washed three times with 200 μl of complete medium per wash, using the same centrifuge settings, and resuspended in the same volume of medium. Washed plates along with the cytostatic assay plates were incubated at 37°C for 48 h. After 48 h, 50 μl of 10× SYBR green I dye (diluted using complete medium from a 10,000× DMSO stock) was added and the plates were incubated for an additional 1 h at 37°C to allow DNA intercalation. Fluorescence was measured at 538 nm (485-nm excitation) using a Spectra GeminiEM plate reader (Molecular Devices, Sunnyvale, CA) fitted with a 530-nm long-pass filter. Linear standard curves of measured fluorescence versus known parasitemia were prepared immediately prior to plate analysis. Background controls included fluorescence from uninfected red blood cells. Data were analyzed using Microsoft Excel 2007 software, and IC_{50} and LD_{50} values were obtained from sigmoidal curve fits to percent growth/survival-versus-drug concentration data using SigmaPlot (version 11.0) software. Reported IC_{50}s are the average of three independent assays, with each assay conducted in triplicate (nine determinations total) and reported ± the standard error of the mean. LD_{50} values are the average of two independent assays, with each assay conducted in triplicate (six determinations total).

VAR calculations. Vacuolar accumulation ratio (VAR) calculations were done using the Henderson-Hasselbalch equation (49, 50) (see equation 2 below) with the external pH at 7.33 and the DV pH at either 5.2 or 5.6 (45). Our calculations also assume that (i) charged (protonated) drugs are $>10^5$-fold less membrane permeant than neutral drugs and (ii) initial rapid accumulation is not limited by binding to the drug target(s):

$$\frac{[\text{drug}]_V}{[\text{drug}]_E} = \frac{1 + 10^{(\text{pKa}_1 - \text{pH}V)} + 10^{(\text{pKa}_1 + \text{pKa}_2 - 2\text{pH}V)} + 10^{(\text{pKa}_1 + \text{pKa}_2 + \text{pKa}_3 - 3\text{pH}V)}}{1 + 10^{(\text{pKa}_1 - \text{pH}E)} + 10^{(\text{pKa}_1 + \text{pKa}_2 - 2\text{pH}E)} + 10^{(\text{pKa}_1 + \text{pKa}_2 + \text{pKa}_3 - 3\text{pH}E)}}$$

where *V* denotes DV, *E* denotes external (blood), and pKa_1, pKa_2, and pKa_3 correspond to titratable N on the CQ analogues. DV-scaled *in vivo* activities for drugs were obtained by multiplying the raw antiplasmodial IC_{50}s and LD_{50}s by the corresponding calculated VAR values.

RESULTS

The broad FPIX absorbance peak observed in the absence of SDS, characteristic of the μ-oxo dimer (51), exhibits maximum λ (λ_{max}) at 389 nm (Fig. 3A, arrow 2), with a shoulder at 359 nm

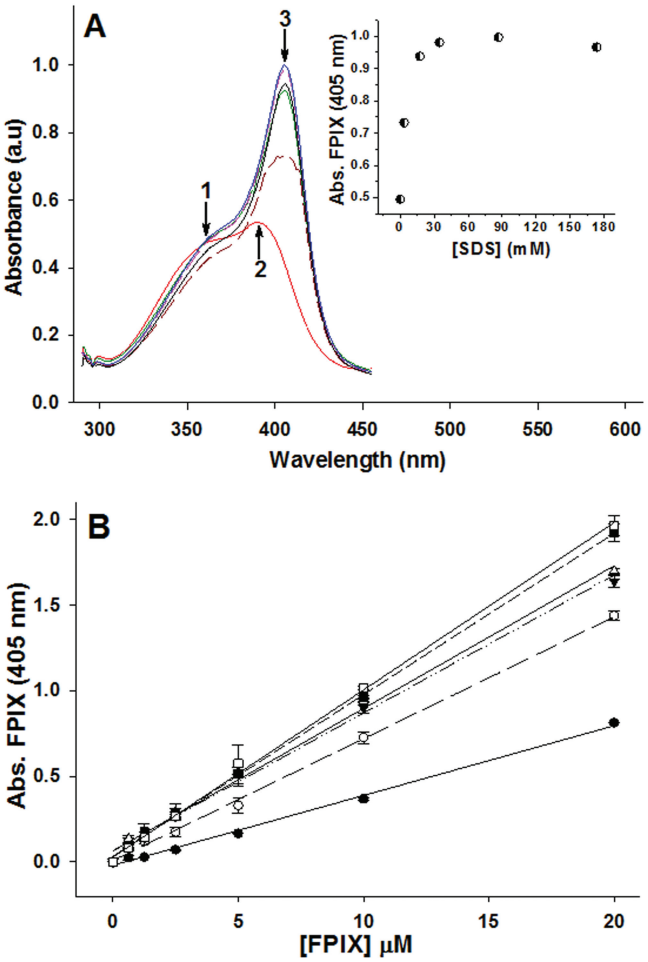

FIG 3 (A) SDS effects on the absorbance spectrum of FPIX. Increasing amounts of SDS were titrated into a cuvette containing 10 μM FPIX while the absorbance spectrum was recorded after each addition. Results are shown for no SDS (red), 0.1% (3.47 mM) SDS (brown), 0.5% (17.3 mM) SDS (green), 1% (34.7 mM) SDS (black), 2.5% (86.7 mM) SDS (blue), and 5% (173 mM) SDS (pink). (Inset) Peak height at 405 nm versus SDS concentration. a.u., absorbance units. (B) Effect of SDS on the concentration-dependent absorbance (Abs.) of FPIX in the 96-well plate format. Results are shown for no SDS (●, $R^2 = 0.996$), 0.1% (3.47 mM) SDS (○, $R^2 = 0.988$), 0.5% (17.3 mM) SDS (▼, $R^2 = 0.992$), 1% (34.7 mM) SDS (■, $R^2 = 0.996$), 2.5% (86.7 mM) SDS (□, $R^2 = 0.998$), and 5% (173 mM) SDS (Δ, $R^2 = 0.999$). Increasing the concentration of SDS increases the absorbance of FPIX to a maximum at ~2.5% SDS. Each data point is an average of three independent measurements, each performed in triplicate (9 determinations total).

(Fig. 3A, arrow 1). We found that simple titration of the μ-oxo dimer with SDS results in a red shift of the FPIX Soret band from 389 nm to 405 nm (Fig. 3A, arrow 3), as well as a concentration-dependent increase in absorbance. This is presumably because upon addition of SDS at concentrations above the critical micelle concentration, free μ-oxo dimeric heme is converted to its monomeric form (52), generating the λ_{max} shift to 405 nm and a concomitant increase in the extinction coefficient to 99,690 (M^{-1} cm^{-1}). This effect is also easily measured in 96-well plate format (Fig. 3B), and the linear increase in absorbance then allows for calibration of free FPIX at a known SDS concentration. That is, conversion of FPIX to Hz can be quantified via simple addition of SDS, without plate-washing steps.

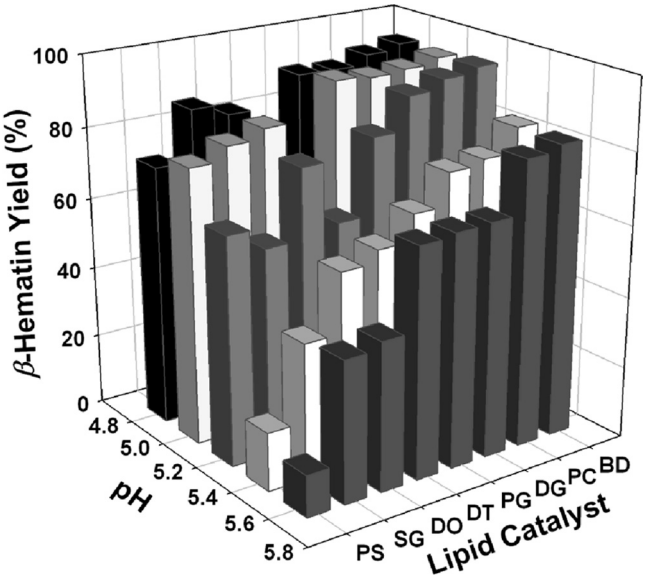

FIG 4 Optimization of lipid catalyst. Comparison of the Hz (β-hematin) catalytic efficiency of PS (L-α-phosphatidyl-L-serine), SG (1-monostearin, sMAG), DO (1,2-diolyl-*rac*-glycerol [18:1, *cis*-9]), DT (1,2-dioctanoyl-*sn*-glycerol-3-PC), PG (1-monopalmitin, pMAG), DG (1,2-dipalmitoyl-*sn*-glycerol-3-PC), PC (L-α-phosphatidylcholine), and BD (blend, meaning an equimolar mixture of PC, pMAG, and sMAG resulting in 1 mM/well final concentration). FPIX (100 μM) was incubated in 1 M propionate buffer (at the different pH values) at 37°C in the presence of 1 mM the corresponding lipid. The amount of Hz formed in the corresponding lipid wells (average of triplicate wells) was quantified relative to that for a lipid-free control after a 16-h incubation period. The 100% Hz yield was calculated via equation 1, with the sample absorbance being that of 100 μM FPIX.

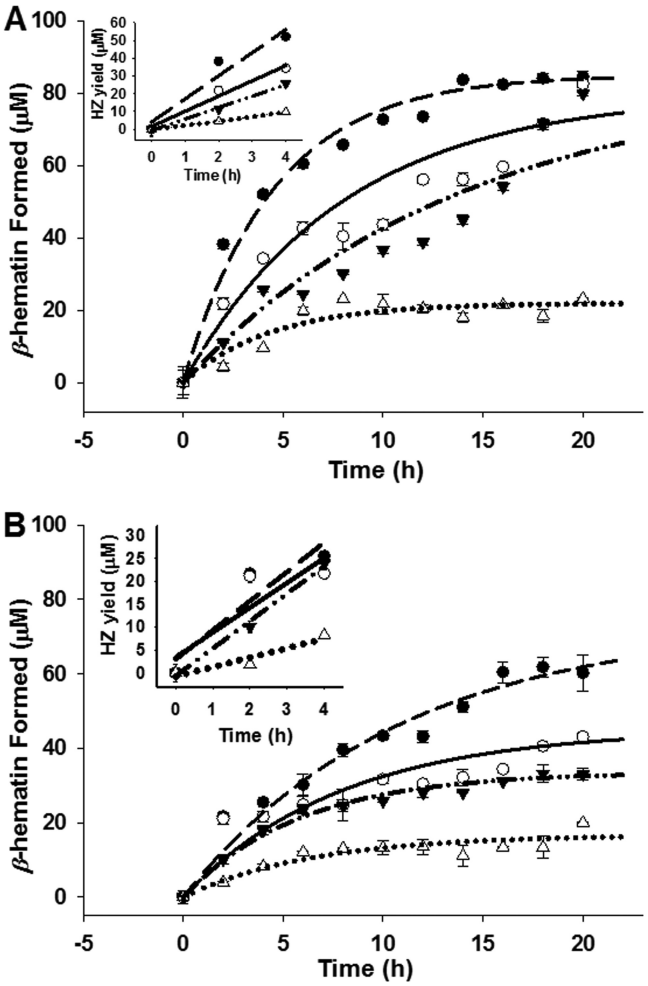

FIG 5 pH-dependent kinetics for the production of Hz (β-hematin) in the presence of PC (●), pMAG (○), or sMAG (▼) or the absence of a catalyst (Δ). Sonicated lipids were incubated at 37°C with 100 μM FPIX in 200 μl of propionate buffer for 16 h at pH 5.2 (A) and pH 5.6 (B). Curve fitting was performed with SigmaPlot (version 10.0) software using the equation $y = a(1 - b^x)$. (Insets) The corresponding initial rate plots from time zero (t_0) to 4 h (t_4) (Table 1). Inset data are fit to linear regressions, and the initial rates were extracted from the slopes. Each data point is an average of three independent measurements, each performed in triplicate (9 determinations total).

To develop an assay that takes advantage of this observation and that also mimics formation of Hz *in vivo* at physiological temperature, pH, and ionic strength, we screened the catalytic abilities of various lipids that are suggested from recent reports to reside within the DV (11, 28). We systematically compared the catalytic efficiency of PC to that of other lipids and mono- or diacyl glycerols (Fig. 4). At physiological temperature, catalysis by PC was comparable to if not better than that found for all other lipids tested, including a blend of PC, pMAG, and sMAG (Fig. 4, BD). We also found that lipid-catalyzed formation of Hz is pH dependent, with the strongest pH dependence found for PS and the weakest found for PC and the PC-pMAG-sMAG blend. More acidic aqueous conditions favor formation of the heme head-to-tail dimer (20); thus, acceleration of Hz formation at lower pH is expected.

We selected PC as the catalyst for additional work because it performed similarly to the blend yet is less expensive and more easily handled. The optimal FPIX concentration was determined to be 100 μM, since this provides a wide dynamic range (>0.6 absorbance unit), as it is converted to Hz over approximately 16 h (see below). Also, under control assay conditions, conversion of 100 μM FPIX to Hz was near 100% (see below).

We next compared the kinetics of Hz formation at 37°C with PC, pMAG, or sMAG as catalysts and at two different pHs that correspond to extremes in DV pH that have been measured for various strains of *P. falciparum* (45) (Fig. 5; Table 1). Again, PC was found to be the most efficient catalyst at either pH, and Hz formation appeared to plateau at about 16 h. We calculated initial rates of Hz formation and noted that at pH 5.2, PC catalysis was 1.5-, 2-, and 5-fold faster than that with pMAG, sMAG, and the control (no lipid), respectively, and that the rate for PC-catalyzed Hz formation in this assay was very similar to that defined for the rate of Hz growth in live parasites (11).

TABLE 1 Initial rates of production of Hz in the presence of PC, pMAG, and sMAG and in the absence of lipid catalysts

Catalyst	Initial rate[a] (M s^{-1} [10^{-8}])	
	pH 5.2	pH 5.6
No lipid	0.67	0.57
PC	3.61	1.77
pMAG	2.39	1.51
sMAG	1.78	1.66

[a] Initial rates were calculated within the first 4 h of the reaction (see insets in Fig. 5).

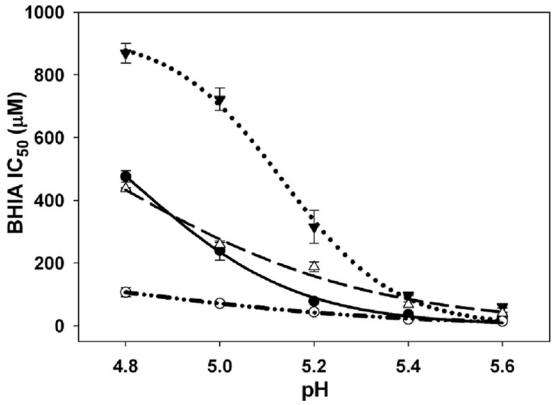

FIG 6 Effect of pH on the Hz inhibition (β-hematin inhibitory activity [BHIA]) IC_{50} of known antimalarial drugs: CQ (●), AQ (○), QN (▼), and QD (Δ). Experiments were performed at 37°C in a 16-h assay. Each data point (± SD) is the average of three independent measurements, each performed in triplicate (9 determinations total) at the corresponding pH.

Using this standardized assay, we quantified inhibition of Hz formation by common antimalarials (CQ, QN, QD, and AQ) at several pHs. Overall, similar to other studies (19, 22, 25), we found that potencies were AQ > CQ ≈ QD > QN across the range of pHs (Fig. 6). We noted that different absolute IC_{50}s were obtained at the same pH when the identity of the lipid catalyst was changed (Table 2) but that the trends for the drugs remained similar. For CQ and AQ, the differences observed when PC versus pMAG catalysts were used were relatively small (2- to 3-fold); however, interestingly, QN and QD IC_{50}s were more perturbed by altering the lipid composition. This is consistent with the differences in CQ versus QN lipid partitioning behavior noted earlier (52).

It has previously been suggested that Hz inhibition and antiplasmodial potency are well correlated (19). However, another study observed that upon correction for different levels of DV accumulation, the linear correlation existed only for CQS strains (21). In both of these studies, the nonphysiological Hz formation conditions and the wide structural diversity of the examined drugs complicate interpretation. We thus tested for a possible correlation between inhibition and antiplasmodial activity using a series of CQ analogues that are structurally similar yet span a wide range of antiplasmodial IC_{50}s and LD_{50}s (Fig. 1; see Table S1 in the supplemental material) (24, 41–43). These analogues also span the effective monobasic, dibasic, and tribasic character and thus diverge in calculated VARs (see Materials and Methods). When Hz inhibition for these compounds was plotted against the antiplasmodial IC_{50} determined versus live merozoite culture, we observed a good correlation when antiplasmodial activity for either CQS ($R^2 = 0.653$) or CQR ($R^2 = 0.639$) strains was tabulated (Fig. 7A and B). However, importantly, when LD_{50} was plotted versus Hz inhibition, these correlations vanished (Fig. 7C and D).

As described earlier (24), replacement of the anilinal N by S or O for some of these compounds significantly lowers the quinolinal N pK_a (to values near those seen for QN or QD; see reference24). *In vivo* antiplasmodial IC_{50}s are presumably defined, in part, by the fold accumulation of the drug at the site of Hz formation (i.e., the acidic DV interior). We therefore scaled antiplasmodial IC_{50}s and LD_{50}s by multiplying by the calculated VARs for each molecule, such that the *in vivo* IC_{50}s were normalized to predicted vacuolar accumulation (see Materials and Methods). However, this did not improve the correlation between either IC_{50} or LD_{50} and Hz inhibition (data not show).

LD_{50} versus IC_{50} data highlight interesting trends for the cytocidal and cytostatic activities observed in the correlation analysis (Fig. 7). For CQ, CQR strain Dd2 was ~10-fold resistant by IC_{50} but ~140-fold resistant by LD_{50} (48) (see Table S1 in the supplemental material). In contrast, AQ has low-nM LD_{50}s, with no significant differences for HB3 versus Dd2 (48). Interestingly, for compounds 1 and 7, Dd2 is hypersensitive by IC_{50} (more sensitive than CQS strain HB3) but is either slightly resistant relative to HB3 (compound 1) or has sensitivity similar to that of HB3 (compound 7) when potency is quantified by LD_{50}. Dd2 is hypersensitive to compounds 6 and 9 by LD_{50} but is resistant to compounds 2 to 5 and 8. Interestingly, some compounds with high IC_{50}s (low cytostatic activity) are more active by LD_{50} (high cytocidal potency) (compounds 7 to 9). Overall, then, the good correlation between Hz inhibition and IC_{50}, with a lack of a correlation between Hz inhibition and LD_{50} for the same drugs, spans a range of CQ compound behavior for CQS versus CQR strains.

DISCUSSION

We report a more physiologically relevant high-throughput assay for quantifying inhibition of Hz formation and test how cytostatic (IC_{50}) versus cytocidal (LD_{50}) activities of CQ and CQ analogues correlate with Hz inhibition. Consistent with most data from other Hz formation assays, we found that Hz inhibition measured under physiological conditions decreases for all drugs examined upon decreasing pH. Presumably, more acidic conditions require a higher drug concentration to inhibit crystal growth because crystallization is accelerated and also because the solubility of precrystalline heme intermediates to which drugs bind is decreased at these pHs. We found that the efficiency of PC in catalyzing Hz formation is comparable to if not better than the efficiency of catalysis by monoacylglycerols, diacylglycerols, and other lipids. All lipids that we tested are found in DV lipid nanospheres harboring nascent Hz crystals, but it is currently not known specifically which of the lipids accelerates the Hz formation that presumably occurs at these nanospheres (11, 28). Our data suggest that all known components of these nanospheres are excellent catalysts.

We used this assay to test previously hypothesized correlations between Hz inhibition and the antiplasmodial IC_{50} in order to ascertain if more close-to-physiological conditions for Hz formation modified those conclusions. Dorn et al. (19) were the first to directly test the hypothesis that antiplasmodial activity was correlated with Hz inhibition by examining a small set of common antimalarials (including quinoline methanols, 4-aminoquinolines, acridines, and nonquinolines). Although Cohen (53) and

TABLE 2 IC_{50} for Hz inhibition at pH 5.2 for common antimalarials in the presence of PC, pMAG, or sMAG

Compound	BHIA IC_{50} (μM)[a]		
	PC	pMAG	sMAG
CQ	67.7	22.4	34.9
AQ	25.4	11.7	16.5
QN	237	59.8	131
QD	111	12.6	36.2

[a] PC, pMAG, or sMAG were present at 1 mM. IC_{50}s were determined using a 16-h endpoint assay at 37°C. BHIA, β-hematin inhibitory activity.

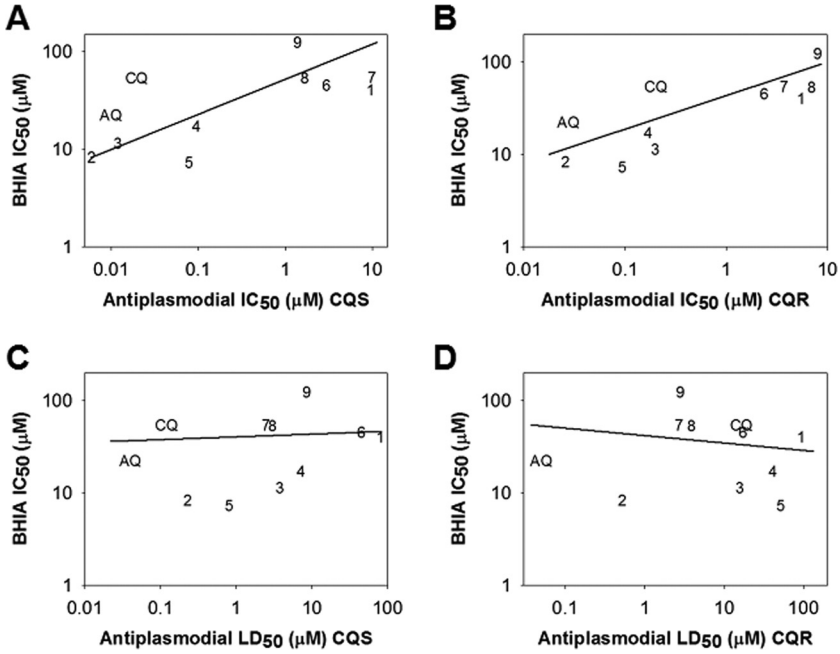

FIG 7 Correlation plots between the Hz inhibition (β-hematin inhibitory activity [BHIA]) IC_{50} and antiplasmodial activities against HB3 (A, C) or Dd2 (B, D) for a series of CQ analogues. Best-fit plots of the data were generated by the least-squares method using SigmaPlot software. (A) Plot of BHIA IC_{50} versus antiplasmodial IC_{50} for CQS HB3 parasites ($R^2 = 0.653$); (B) plot of BHIA IC_{50} versus antiplasmodial IC_{50} for CQR Dd2 parasites ($R^2 = 0.639$); (C) plot of BHIA IC_{50} versus antiplasmodial LD_{50} for HB3 parasites ($R^2 = 0.015$); (D) plot of BHIA IC_{50} versus antiplasmodial LD_{50} for Dd2 parasites ($R^2 = 0.057$). IC_{50} and LD_{50} values are those found in Table S1 in the supplemental material.

Macomber and Spintz (54) proposed that heme was a target for quinoline antimalarial drugs more than 30 years before this study, results from Dorn et al. (19) have been crucial for exploring the molecular pharmacology of antimalarial drugs and have been highly influential in guiding additional antimalarial drug development. Using a CQS strain (NF54), these authors observed a linear correlation between the potency of Hz inhibition and antiplasmodial IC_{50} for common antimalarials, which are thus now known as "heme-acting" antimalarial drugs. Hawley et al. (21) further investigated this concept using CQS (3D7) and CQR (K1) strains and a similar series of quinoline methanols, 4-aminoquinolines, and acridines. In contrast to Dorn and coworkers (19), these authors observed no apparent correlation between the two activities when comparing raw IC_{50} data for either CQS or CQR strains. However, after VAR correction, Hawley and coworkers (21) did observe a correlation, but only for the CQS strain. A third study by Kaschula et al. (38) also observed a correlation between the two activities, but again, only when the antiplasmodial IC_{50} was scaled to the relative VAR. In this study, the authors utilized a series of 2-carbon 4-aminoquinoline derivatives with variable functionalities at position 7.

There are logical explanations for these differing results. First, the use of a nonhomologous series of compounds (e.g., quinolines versus acridines) that have very different bioavailability profiles, as well as the nonphysiological conditions of the Hz formation assays that were used, makes interpretation more complex. There are multiple Hz precursors (FPIX monomer, μ-oxo dimer, and head-to-tail dimer) against which this range of pharmacophores interacts (13, 14, 17, 51, 52, 55), and the relative effectiveness of monomeric heme-drug versus dimeric heme-drug complexes for inhibiting Hz formation likely differs.

A complete understanding of the correlation between antiplasmodial IC_{50} activity and Hz inhibition requires more detailed chemical information on the nature of solid-state aggregates of heme and quinoline compounds. Earlier studies clearly showed that the solubilities of monomeric and dimeric forms of FPIX are dramatically affected by the presence of quinolines (51, 56), that CQ and other quinoline antimalarials bind with different affinities to monomeric versus dimeric FPIX (14, 17, 51), and that the solubility of drug-heme complexes in hydrophobic phase may be more relevant to Hz inhibition potency (11, 52). Taken together, these data show that quinoline drug-heme interactions are significantly more complex than simple aqueous equilibria predict.

Regardless, the principle conclusion of Dorn et al. (19) has continued to strengthen the notion that the site of quinoline antimalarial drug action must be the DV, where the drug then binds to free heme to prevent Hz crystallization. Therefore, altered DV biochemistry that reduces drug-heme interaction must be the cause of resistance to these drugs, a prediction that has been validated by studies on the function of mutant *P. falciparum* chloroquine resistance transporter (PfCRT; a DV membrane protein), which causes an elevated CQ IC_{50} in *P. falciparum* malaria (57).

Data in the present paper reveal a good correlation between antiplasmodial IC_{50}s and Hz inhibition across a series of CQ analogues with a wide range of IC_{50}s (Fig. 7), similar to the conclusions of Dorn et al. (19). Using Hz inhibition quantified under physiological conditions with lipid catalyst, our data also suggest that the correlation is not necessarily improved when estimated VARs or other pharmacokinetic parameters (e.g., pKa, octanol/water partitioning, and water diffusion; see Table S1 in the supplemental material) are applied to the data set (data not shown;

see Materials and Methods and Table S1 in the supplemental material). Regardless, although the IC_{50s} of our set of CQ analogues span a very wide range, they are not necessarily representative of all CQ analogues studied to date, and correlation between antiplasmodial IC_{50} and Hz inhibition IC_{50} for quinoline antimalarials may be dependent (at least in part) upon the specific drugs that are assessed (see the accompanying paper [40]).

Critically, however, and in distinct contrast to the correlation with the IC_{50}, there is a complete lack of correlation between the Hz inhibition IC_{50} and antiplasmodial LD_{50} for the same series of CQ analogues (Fig. 7C and D). This is similar to conclusions reached previously with a smaller set of quinoline methanol compounds, including 9-epimers of quinine and quinidine (see the accompanying paper [40]). Our test series of CQ analogues were chosen because they exhibit a wide range of cytostatic and cytocidal activities (see Results and Table S1 in the supplemental material) and also show a variety of other interesting trends, as noted in Results. Strain Dd2 resistance to CQ is 10-fold by IC_{50} but 140-fold by LD_{50}, suggesting that a significantly different pharmacology may be relevant to understanding the different modes of action for CQ (48). AQ does not exhibit significant differences in IC_{50} and LD_{50} activity for HB3 versus Dd2 and is quite potent (low nM) by both antiplasmodial measurements (see Table S1 in the supplemental material). This suggests to us that the cytocidal targets for CQ versus AQ may differ and/or that the mechanism of CQ cytocidal resistance is distinct from that for AQ.

With these results, we suggest that three critical principles are becoming increasingly apparent: (i) potent IC_{50} activity can but does not always indicate potent LD_{50} activity for quinoline antimalarials, (ii) resistance to cytostatic drug effects does not always correlate with resistance to cytocidal drug effects, and (iii) for CQ and CQ analogues, the ability to inhibit Hz formation correlates strongly with IC_{50} potency but not with LD_{50} potency. The large differences between IC_{50} and LD_{50} measures of activity against HB3 and Dd2 parasites suggest that the molecular mechanisms of resistance to the cytostatic and cytocidal effects of quinoline antimalarial drugs likely differ (see also reference58). For CQ, cytostatic resistance (elevated IC_{50}) is mediated by PfCRT and/or *P. falciparum* multidrug resistance protein (PfMDR1) mutations that alter the electrochemical potential-driven DV transport of the protonated drug (57, 59–63) and, hence, access to heme. However, mounting experimental evidence (48, 58) suggests the possibility of additional (non-DV) cytocidal targets for this class of drugs, which then predicts the possibility of additional cytocidal resistance mechanisms that are mechanistically distinct from cytostatic resistance mechanisms (64).

In sum, we have used physiological assay conditions and analysis of a homologous series of CQ analogues that possess a wide range of pharmacokinetic properties and antiplasmodial activities to test the correlation between antiplasmodial activity and inhibition of Hz. All compounds were screened side by side under the same conditions, using an assay incorporating physiological temperature, ionic strength, and lipid catalyst. The results, coupled with other recent data (48, 58), strongly support the idea that Hz inhibition is the predominant target for the cytostatic activity of CQ and related compounds but not the predominant target for cytocidal activity.

ACKNOWLEDGMENTS

This work was supported by NIH grants AI045957 (to P.D.R.) and AI060792 (to A.C.D.D. and P.D.R. and to C. Wolf, Georgetown University).

We thank Changan Xie for insightful discussions and the C. Wolf laboratory at the Georgetown University Department of Chemistry for providing additional aliquots of compounds 1 to 5.

REFERENCES

1. **World Health Organization.** 2010. World malaria report 2010. World Health Organization, Geneva, Switzerland. http://www.who.int/malaria/publications/atoz/9789241564106/en/index.html.
2. **Cheeseman IH, Miller BA, Nair S, Nkhoma S, Tan A, Tan JC, Al Saai S, Phyo AP, Moo CL, Lwin KM, McGready R, Ashley E, Imwong M, Stepniewska K, Yi P, Dondorp AM, Mayxay M, Newton PN, White NJ, Nosten F, Ferdig MT, Anderson TJ.** 2012. A major genome region underlying artemisinin resistance in malaria. Science **336**:79–82.
3. **Roepe PD.** 2009. Molecular and physiologic basis of quinoline drug resistance in *Plasmodium falciparum* malaria. Future Microbiol. **4**:441–455.
4. **Sa JM, Chong JL, Wellems TE.** 2011. Malaria drug resistance: new observations and developments. Essays Biochem. **51**:137–160.
5. **Barnes KI, Watkins WM, White NJ.** 2008. Antimalarial dosing regimens and drug resistance. Trends Parasitol. **24**:127–134.
6. **Banerjee R, Liu J, Beatty W, Pelosof L, Klemba M, Goldberg DE.** 2002. Four plasmepsins are active in the *Plasmodium falciparum* food vacuole, including a protease with an active-site histidine. Proc. Natl. Acad. Sci. U. S. A. **99**:990–995.
7. **Gamboa de Domínguez ND, Rosenthal PJ.** 1996. Cysteine proteinase inhibitors block early steps in hemoglobin degradation by cultured malaria parasites. Blood **87**:4448–4454.
8. **Yoshida T, Migita TC.** 2000. Mechanism of heme degradation by heme oxygenase. J. Inorg. Biochem. **82**:33–41.
9. **Egan TJ, Combrinck JM, Egan J, Hearne GR, Marques HM, Ntenteni S, Sewell BT, Smith PJ, Taylor D, van Schalkwyk DA, Walden JC.** 2002. Fate of haem iron in the malaria parasite *Plasmodium falciparum*. Biochem. J. **365**:343–347.
10. **Pagola S, Stephens PW, Bohle DS, Kosar AD, Madsen SK.** 2000. The structure of malaria pigment beta-haematin. Nature **404**:307–310.
11. **Pisciotta JM, Coppens I, Tripathi AK, Scholl PF, Shuman J, Bajad S, Shulaev V, Sullivan DJ, Jr.** 2007. The role of neutral lipid nanospheres in *Plasmodium falciparum* haem crystallization. Biochem. J. **402**:197–204.
12. **Tripathi AK, Garg SK, Tekwani BL.** 2002. A physiochemical mechanism of hemozoin (β-hematin) synthesis by malaria parasite. Biochem. Biophys. Res. Commun. **290**:595–601.
13. **de Dios AC, Casabianca LB, Kosar A, Roepe PD.** 2004. Structure of the amodiaquine-FPIX mu-oxo dimer solution complex at atomic resolution. Inorg. Chem. **43**:8078–8084.
14. **de Dios AC, Tycko R, Ursos LMB, Roepe PD.** 2003. NMR studies of chloroquine-ferriprotoporphyrin IX complex. J. Phys. Chem. A **107**:5821–5825.
15. **Egan TJ, Ncokazi KK.** 2005. Quinolines decrease the rate of β-hematin formation. J. Inorg. Biochem. **99**:1532–1539.
16. **Egan TJ, Ross DC, Adams PA.** 1994. Quinoline anti-malarial drugs inhibit spontaneous formation of beta-haematin (malaria pigment). FEBS Lett. **352**:54–57.
17. **Leed A, DuBay K, Sears D, de Dios AC, Roepe PD.** 2002. Solution structures of antimalarial drug-heme complexes. Biochemistry **41**:10245–10255.
18. **Sullivan DJ, Jr, Gluzman IY, Russell DG, Goldberg DE.** 1996. On the molecular mechanism of chloroquine's antimalarial action. Proc. Natl. Acad. Sci. U. S. A. **93**:11865–11870.
19. **Dorn A, Vippagunta SR, Matile H, Jaquet C, Vennerstrom JL, Ridley RG.** 1998. An assessment of drug-haematin binding as a mechanism for inhibition of haematin polymerisation by quinoline antimalarials. Biochem. Pharmacol. **55**:727–736.
20. **Egan TJ, Mavuso WW, Ncokazi KK.** 2001. The mechanism of beta-hematin formation in acetate solution. Parallels between hemozoin formation and biomineralization processes. Biochemistry **40**:204–213.
21. **Hawley SR, Bray PG, Mungthin M, Atkinson JD, O'Neill PM, Ward SA.** 1998. Relationship between antimalarial drug activity, accumulation, and

inhibition of heme polymerization in *Plasmodium falciparum* in vitro. Antimicrob. Agents Chemother. **42**:682–686.
22. **Huy NT, Uyen DT, Maeda A, Trang DT, Oida T, Harada S, Kamei K.** 2007. Simple colorimetric inhibition assay of heme crystallization for high-throughput screening of antimalarial compounds. Antimicrob. Agents Chemother. **51**:350–353.
23. **Kurosawa Y, Dorn A, Kitsuji-Shirane M, Shimada H, Satoh T, Matile H, Hofheinz W, Masciadri R, Kansy M, Ridley RG.** 2000. Hematin polymerization assay as a high-throughput screen for identification of new antimalarial pharmacophores. Antimicrob. Agents Chemother. **44**:2638–2644.
24. **Natarajan JK, Alumasa JN, Yearick K, Ekoue-Kovi KA, Casabianca LB, de Dios AC, Wolf C, Roepe PD.** 2008. 4-N-, 4-S-, and 4-O-chloroquine analogues: influence of side chain length and quinolyl nitrogen p*K*a on activity vs chloroquine resistant malaria. J. Med. Chem. **51**:3466–3479.
25. **Ncokazi KK, Egan TJ.** 2005. A colorimetric high-throughput beta-hematin inhibition screening assay for use in the search for antimalarial compounds. Anal. Biochem. **338**:306–319.
26. **Parapini S, Basilico N, Pasini E, Egan TJ, Olliaro P, Taramelli D, Monti D.** 2000. Standardization of the physicochemical parameters to assess in vitro the beta-hematin inhibitory activity of antimalarial drugs. Exp. Parasitol. **96**:249–256.
27. **Chong CR, Sullivan DJ, Jr.** 2003. Inhibition of heme crystal growth by antimalarials and other compounds: implications for drug discovery. Biochem. Pharmacol. **66**:2201–2212.
28. **Jackson KE, Klonis N, Ferguson DJ, Adisa A, Dogovski C, Tilley L.** 2004. Food vacuole-associated lipid bodies and heterogeneous lipid environments in the malaria parasite, *Plasmodium falciparum.* Mol. Microbiol. **54**:109–122.
29. **Sullivan DJ, Jr, Gluzman IY, Goldberg DE.** 1996. *Plasmodium* hemozoin formation mediated by histidine-rich proteins. Science **271**:219–222.
30. **Egan TJ, Chen JY, de Villies KA, Mabotha TE, Naidoo JJ, Ncokazi KK, Langford McNaughton SJ, Pandiancherii S, Wood BR.** 2006. Hemozoin (beta-hematin) biomineralization occurs by self-assembly near the lipid/water interface. FEBS Lett. **580**:5105–5110.
31. **Fitch CD, Cai GZ, Chen YF, Shoemaker JD.** 1999. Involvement of lipids in ferriprotoporphyrin IX polymerization in malaria. Biochim. Biophys. Acta **1454**:31–37.
32. **Huy NT, Uyen DT, Sasai M, Trang DT, Shiono T, Harada S, Kamei K.** 2006. A simple and rapid colorimetric method to measure hemozoin crystal growth in vitro. Anal. Biochem. **354**:305–307.
33. **Pandey AV, Joshi SK, Tekwani BL, Chauhan VS.** 1999. A colorimetric assay for heme in biological samples using 96-well plates. Anal. Biochem. **268**:159–161.
34. **Pandey AV, Singh N, Tekwani BL, Puri SK, Chauhan VS.** 1999. Assay of beta-hematin formation by malaria parasite. J. Pharm. Biomed. Anal. **20**: 203–207.
35. **Trang DT, Huy NT, Uyen DT, Sasai M, Shiono T, Harada S, Kamei K.** 2006. Inhibition assay of beta-hematin formation initiated by lecithin for screening new antimalarial drugs. Anal. Biochem. **349**:292–296.
36. **Tripathi AK, Gupta A, Garg SK, Tekwani BL.** 2001. In vitro beta-hematin formation assays with plasma of mice infected with *Plasmodium yoelii* and other parasite preparations: comparative inhibition with quinoline and endoperoxide antimalarials. Life Sci. **69**:2725–2733.
37. **Tripathi AK, Khan SI, Walker LA, Tekwani BL.** 2004. Spectrophotometric determination of de novo hemozoin/beta-hematin formation in an in vitro assay. Anal. Biochem. **325**:85–91.
38. **Kaschula CH, Egan TJ, Hunter R, Basilico N, Parapini S, Taramelli D, Pasini DE, Monti D.** 2002. Structure-activity relationships in 4-aminoquinoline antiplasmodials. The role of the group at the 7-position. J. Med. Chem. **45**:3531–3539.
39. **Dinio T, Gorka AP, McGinniss A, Roepe PD, Morgan JB.** 2012. Investigating the activity of quinine analogues versus chloroquine resistant *Plasmodium falciparum.* Bioorg. Med. Chem. **20**:3292–3297.
40. **Gorka AP, Sherlach KS, de Dios AC, Roepe PD.** 2013. Relative to quinine and quinidine, their 9-epimers exhibit decreased cytostatic activity and altered heme binding but similar cytocidal activity versus *Plasmodium falciparum.* Antimicrob. Agents Chemother. **57**:365–374.
41. **Ekoue-Kovi K, Yearick K, Iwaniuk DP, Natarajan JK, Alumasa J, de Dios AC, Roepe PD, Wolf C.** 2009. Synthesis and antimalarial activity of new 4-amino-7-chloroquinolyl amides, sulfonamides, ureas and thioureas. Bioorg. Med. Chem. **17**:270–283.
42. **Iwaniuk DP, Whetmore ED, Rosa N, Ekoue-Kovi K, Alumasa J, de Dios AC, Roepe PD, Wolf C.** 2009. Synthesis and antimalarial activity of new chloroquine analogues carrying a multifunctional linear side chain. Bioorg. Med. Chem. **17**:6560–6566.
43. **Yearick K, Ekoue-Kovi K, Iwaniuk DP, Natarajan JK, Alumasa J, de Dios AC, Roepe PD, Wolf C.** 2008. Overcoming drug resistance to heme-targeted antimalarials by systematic side chain variation of 7-chloro-4-aminoquinolines. J. Med. Chem. **51**:1995–1998.
44. **Lekostaj JK, Natarajan JK, Paguio MF, Wolf C, Roepe PD.** 2008. Photoaffinity labeling of the *Plasmodium falciparum* chloroquine resistance transporter with a novel perfluorophenylazido chloroquine. Biochemistry **47**:10394–10406.
45. **Bennett TN, Kosar AD, Ursos LM, Dzekunov S, Singh-Sidhu AB, Fidock DA, Roepe PD.** 2004. Drug resistance-associated pfCRT mutations confer decreased *Plasmodium falciparum* digestive vacuolar pH. Mol. Biochem. Parasitol. **133**:99–114.
46. **Trager W, Jensen JB.** 1976. Human malaria parasites in continuous culture. Science **193**:673–675.
47. **Bennett TN, Paguio M, Gligorijevic B, Seudieu C, Kosar AD, Davidson E, Roepe PD.** 2004. Novel, rapid, and inexpensive cell-based quantification of antimalarial drug efficacy. Antimicrob. Agents Chemother. **48**:1807–1810.
48. **Paguio MF, Bogle KL, Roepe PD.** 2011. *Plasmodium falciparum* resistance to cytocidal versus cytostatic effects of chloroquine. Mol. Biochem. Parasitol. **178**:1–6.
49. **Hawley SR, Bray PG, O'Neil PM, Park BK, Ward SA.** 1996. The role of drug accumulation in 4-aminoquinoline antimalarial potency. Biochem. Pharmacol. **52**:723–733.
50. **Krogstad DJ, Schlesinger PH.** 1998. A perspective on antimalarial action: effects of weak bases on *Plasmodium falciparum.* Biochem. Pharmacol. **35**:793–798.
51. **Casabianca LB, An D, Natarajan JK, Alumasa JN, Roepe PD, Wolf C, de Dios AC.** 2008. Quinine and chloroquine differentially perturb heme monomer-dimer equilibrium. Inorg. Chem. **47**:6077–6081.
52. **Casabianca LB, Kallgren JB, Natarajan JK, Alumasa JN, Roepe PD, Wolf C, de Dios AC.** 2009. Antimalarial drugs and heme in detergent micelles: an NMR study. J. Inorg. Biochem. **103**:745–748.
53. **Cohen SN, Phifer KO, Yielding KL.** 1964. Complex formation between chloroquine and ferrihaemic acid in vitro, and its effect on the antimalarial action of chloroquine. Nature **202**:805–806.
54. **Macomber PB, Spintz H.** 1967. Morphological effects of chloroquine on *Plasmodium berghei* in mice. Nature **214**:937–939.
55. **Alumasa JN, Gorka AP, Casabianca LB, Comstock E, de Dios AC, Roepe PD.** 2011. The hydroxyl functionality and a rigid proximal N are required for forming a novel non-covalent quinine-heme complex. J. Inorg. Biochem. **105**:467–475.
56. **Ursos LM, DuBay KF, Roepe PD.** 2001. Antimalarial drugs influence the pH dependent solubility of heme via apparent nucleation phenomena. Mol. Biochem. Parasitol. **112**:11–17.
57. **Roepe PD.** 2011. PfCRT-mediated drug transport in malarial parasites. Biochemistry **50**:163–171.
58. **Cabrera M, Paguio MF, Xie C, Roepe PD.** 2009. Reduced digestive vacuolar accumulation of chloroquine is not linked to resistance to chloroquine toxicity. Biochemistry **48**:11152–11154.
59. **Cooper RA, Ferdig MT, Su XZ, Ursos LM, Mu J, Nomura T, Fujioka H, Fidock DA, Roepe PD, Wellems TE.** 2002. Alternative mutations at position 76 of the vacuolar transmembrane protein PfCRT are associated with chloroquine resistance and unique stereospecific quinine and quinidine responses in *Plasmodium falciparum.* Mol. Pharmacol. **61**:35–42.
60. **Cooper RA, Lane KD, Deng B, Mu J, Patel JJ, Wellems TE, Su X, Ferdig MT.** 2007. Mutations in transmembrane domains 1, 4, and 9 of the *Plasmodium falciparum* chloroquine resistance transporter alter susceptibility to chloroquine, quinine, and quinidine. Mol. Microbiol. **63**:270–282. (Erratum, Mol. Microbiol. **64**:1139–1148.)
61. **Ferdig MT, Cooper RA, Mu J, Deng B, Joy DA, Su XZ, Wellems TE.** 2004. Dissecting the loci of low-level quinine resistance in malaria parasites. Mol. Microbiol. **52**:985–997.
62. **Sidhu AB, Valderramos SG, Fidock DA.** 2005. *pfmdr1* mutations contribute to quinine resistance and enhance mefloquine and artemisinin sensitivity in *Plasmodium falciparum.* Mol. Microbiol. **57**:913–926.
63. **Sidhu AB, Verdier-Pinard D, Fidock DA.** 2002. Chloroquine resistance in *Plasmodium falciparum* malaria parasites conferred by *pfcrt* mutations. Science **298**:210–213.
64. **Sinai AP, Roepe PD.** 2012. Autophagy in apicomplexa: a life sustaining death mechanism? Trends Parasitol. **28**:358–364.